

# EXPERIMENTAL AND COMPUTATIONAL INVESTIGATION OF THE PERFORMANCE OF A MICRO-ION THRUSTER

Richard Wirz\*, James Polk†, Colleen Marrese†, Juergen Mueller†

\*California Institute of Technology, Pasadena, CA 91106, USA

†Jet Propulsion Laboratory, California Institute of Technology, 4800 Oak Grove Drive, Pasadena, CA 91109, US

Abstract – A micro-ion thruster assembly with a characteristic diameter of 3-cm has been developed at JPL for testing and optimization of various system parameters. The effectiveness of the chamber magnetic field to utilize the exit grids is investigated in this paper by using experimentally obtained beam profiles to computationally determine the ion density just inside the chamber. A method is presented for determining the beam profile at the grid exit from two downstream beam profiles. The experimental and computational results show that the micro-ion thruster design discussed herein yields favorable beam and ion profiles. However, the calculated values of ion and neutral density in the chamber, along with preliminary computational results, show that considerable increases to thruster performance may be attained with relatively minor design and operational modifications.

## Nomenclature

### Variables

$F$  = flatness parameter [See Equation (8)]  
 $I_{sp}$  = specific impulse  
 $j$  = current density  
 $J$  = current  
 $k$  = Boltzmann's constant  
 $m$  = mass  
 $\dot{m}$  = mass flow rate  
 $n$  = particle density  
 $\dot{n}$  = particle flow rate [equivalent Amperes]  
 $p$  = electron pressure =  $n_e kT_e$   
 $P$  = pressure  
 $q$  = electric charge  
 $Q$  = collision cross-section  
 $r$  = distance from thruster axis  
 $R$  = beam radius  
 $t$  = time  
 $T$  = temperature  
 $v$  = velocity  
 $V$  = voltage  
 $z$  = axial distance

$\varepsilon_B$  = beam ion energy cost  
 $\delta$  = open area fraction  
 $\phi$  = electric potential  
 $\eta$  = efficiency  
 $\lambda$  = mean free path

### Subscripts

$B$  = beam  
 $CEX$  = charge exchange  
 $ch$  = vacuum chamber

$D$  = discharge  
 $e$  = electron  
 $i$  = ion  
 $prop$  = propellant  
 $o$  = neutral atom  
 $\infty$  = ambient

## Introduction

### Background and Motivation

A micro-ion thruster offers a unique combination of high efficiency, high specific impulse ( $I_{sp}$ ), benign propellants, and low thrust with the capability for continuous operation for a variety of future space missions<sup>1</sup>. Recent results have shown that attractive performance is possible for micro-ion thrusters<sup>2</sup>. It was shown for micro-ion thruster with a 3cm diameter that the shape of the discharge magnetic field and the discharge chamber geometry greatly affects the performance of the thruster. However, the performance related to the micro-machined grids and the chamber ion and neutral densities had not been investigated.

Analyzing the beam current density profiles in the thruster plume one can assess the performance of the grids and the discharge chamber. The beam profiles allow many characteristics of a thruster to be determined, including: beam divergence, grid utilization, uneven grid wear, and overall thruster performance. Statistical and qualitative correlations have been shown to exist between the beam profile at the grid exit plane and the discharge chamber ion density profile near the grids<sup>3,4</sup>. Therefore, the effectiveness of a discharge chamber and exit grid

design may be considered strongly dependent on the discharge ion density profile near the grids and its relationship to the beam profile.

### Objective

This paper presents a method for determining the discharge chamber ion density of a micro-ion thruster just inside the exit grids by considering the beam profile at the exit plane. At the micro-ion thruster scale, the beam measurements cannot be taken sufficiently close to the grid exit plane without significant proximity effects and electrical shorting. Consequently, a technique for projecting downstream beam profile data back to the grid exit plane is discussed. In addition, a method for quantitatively assessing the grid area utilization is developed. With this information the micro-ion thruster discharge chamber performance, grid utilization, beam divergence, and efficiencies can be more thoroughly understood.

### Experimental Setup

The micro-ion thruster and testing facility used in this investigation are discussed in Reference 2. The thruster faces vertically upward and a small faraday probe oriented parallel to the thruster axis was used to make linear sweeps across the thruster plume at various heights. The thruster configuration tested herein is a double ring cusp design with a length-to-diameter ratio of 1, as shown in Reference 2. Flat micro-machined molybdenum exit grids with circular holes were used for the grid accelerator system.

### Theory and Analysis

#### Beam Divergence and Charge Exchange

The following section discusses the relationships used to determine the effects of beam divergence and charge exchange collisions in the thruster plume.

Quasi-neutral ion beam plasma, such as those used in this investigation, may be considered isothermal and the spatial variation of the plasma density and potential follows the barometric law<sup>5</sup>.

$$n(\vec{r}) = n_o \exp\left[\frac{q\phi(\vec{r})}{kT}\right] \quad (1)$$

The motion of the beam ions is governed by the ion momentum equation.

$$m_i \frac{d\vec{v}_i}{dt} = -q\nabla\phi \quad (2)$$

The barometric law, Equation (1), is derived from the momentum balance equation for a stationary electron gas

$$m_e \frac{d\vec{v}_e}{dt} = q\nabla\phi - \nabla p = 0 \quad (3)$$

for constant  $T$  where the electron pressure is  $p = nkT$ . Therefore, by combining Equations (2) and (3), and assuming isothermal conditions, we can relate the motion of the beam ions to the beam plasma density by

$$m_i \frac{d\vec{v}_i}{dt} = -kT \frac{\nabla n}{n} \quad (4)$$

The beam divergence is then governed by Equation (4) and the radial distribution of the ion-optical properties of the exit grids.

It is important to determine the amount of the beam current that is lost due to charge exchange (CEX) interactions of the beam ions with the ambient xenon neutrals. The charge exchange losses in the beam will increase with distance from the thruster and will affect the accuracy of beam profile measurements at increasing distances from the grid exit plane. The loss of beam current  $J_B$  directed perpendicular to a slab of xenon neutrals with density  $n_o$  of xenon neutrals and thickness  $dx$  may be expressed as

$$dJ_B = -J_B n_o Q_{CEX} dz \quad (5)$$

Since the mean free path for CEX collisions is  $\lambda_{CEX} = 1/(n_o Q_{CEX})$ , the beam current at an axial location  $z$  from the exit plane of the thruster is

$$J_B(z) = J_B(0) \exp\left[\frac{-z}{\lambda_{CEX}}\right] \quad (6)$$

Neglecting charge exchange losses, the total beam current may be approximated from a known beam profile by integrating the measured beam current densities over the radial extent of the profile by

$$J_B = \int_0^R j_B(r) 2\pi r dr \quad (7)$$

#### Chamber Ion Density

A 2-D ion optics code developed at JPL, CEX2D, can evaluate the performance of a given grid geometry over a wide range of discharge chamber densities. By using this code, the ion density profile just inside the chamber can be determined if the beam profile near the grid exit plane is known.

Significant variations in the spacing between the exit grids can occur due to the large potential gradient between the grids and the thermal expansion of the grid material during thruster operation. An analytical model can be used to determine the deflection of the plates due to thermal expansion<sup>6</sup>. The results of this analytical model may be coupled with a numerical model to include the effects of electrostatic attraction between the grids to determine the grid deflection as a function of radius<sup>7</sup>. The results of these deflections are used in the aforementioned ion optics code for more accurate grid spacing values.

### Grid Utilization

The utilization of the exit grids can be assessed by relating the beam profile and the profile of the neutral loss rate through the grids. The neutral loss is usually considered constant for all areas of the grids; however, the beam profile may contain drastic variations along the radial extent of the thruster exit. One way to quantitatively assess these variations is to use the flatness parameter,  $F$ , which is given by<sup>8</sup>

$$F = \frac{\int_0^R j_B(r) 2\pi r dr}{\pi^2 j_{Bmax}} \quad (8)$$

As discussed in Beattie, a low flatness parameter value reveals potential lifetime issues and poor grid utilization.

The rate of neutral loss through the grids may be calculated by the relation

$$\dot{n}_g = \dot{n}_{prop} - J_B \quad (9)$$

where  $\dot{n}_g$  and  $\dot{n}_{prop}$  are expressed in equivalent amperes. Using the neutral loss rate and grid dimensions, neutral density inside the discharge chamber is approximated using free molecular flow through a sharp-edged orifice<sup>9</sup>

$$n_o = \frac{4\dot{n}_g}{ev_o A_g \delta_o} \quad (10)$$

The neutral densities calculated by Equation (10) were used in the 2-D ion optics code.

## Results

### Experimental Results

The faraday probe was used to take beam profiles at distances of 8 and 23mm from the exit plane of the thruster. Profiles were taken at multiple thruster operating conditions within the ranges shown in Table 1. The primary upper limitation to the ranges in Table 1 is due to the desire to keep the temperature of the samarium cobalt magnets below their maximum operating temperature of 350°C.

Table 1. Thruster Operation Ranges

Parameter	Range*
$V_B$	700 – 1126 V
$V_D$	23.5 – 29 V
$J_B$	7 – 23 mA
$J_D$	70 - 400 mA
$\dot{n}_{prop}$	0.17 – 0.29 mg/s
Power*	14 – 25 W
$P_{ch}$	6.3E-6 – 2.0E-5 Torr
T	180 – 330°C
Thrust	0.4 – 1.0 mN
$I_{sp}$	1764 – 2934 s
$\epsilon_B$	450 – 650 eV/ion
$\eta_u$	0.5 – 0.75
$\eta_{tot}$	0.31 – 0.5

\*Values ignore doubly-charged ions and cathode input power as discussed in Reference 2.

An example of beam profiles obtained using probe measurements is shown in Figure 1. The total beam current measured from the current emitted by the neutralizer cathode correlated very well with the total beam current obtained by integrating over the beam profiles with Equation (7).

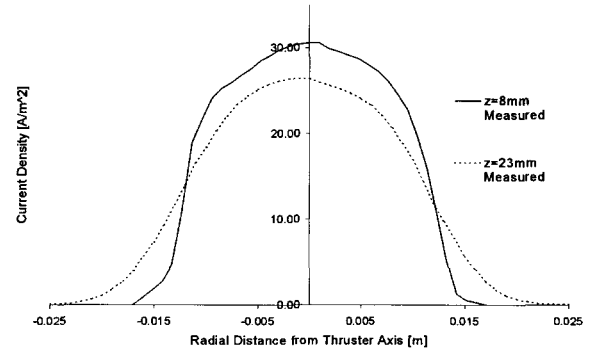


Figure 1. Measured Beam Profiles

The axial depreciation in beam current due to charge exchange losses was calculated at a

distance of 23mm from the thruster exit plane using Equation (6). At the highest measured ambient neutral gas pressure and operating voltage, the change in beam current for both singly- and doubly-charged ions due to charge exchange was only 0.6% and 0.4% respectively. Therefore, for the probe distances used, it is reasonable to ignore the effect of charge exchange collisions.

### Exit Plane Beam Profiles

A simple finite-difference model was developed that uses beam profiles measured at two axial locations downstream of the thruster exit to predict the profile at the thruster exit plane. The model uses Equation (4) to describe the beam divergence due to the downstream plasma and correlates the known downstream density profiles to determine the radial distribution of ion optical properties of the exit grids.

The predicted exit plane profile for the data presented in Figure 1 is shown in Figure 2. The model is matched exactly with the measured profile at 8mm. The beam divergence due to the ion optics is approximated so that the downstream profile predicted by the model matches the experimentally measured downstream profile at the same axial location within 5% of the beam flatness as calculated by Equation (8). The electron temperature of the downstream plasma was measured to be approximately 2.7eV for most operating conditions<sup>10</sup>.

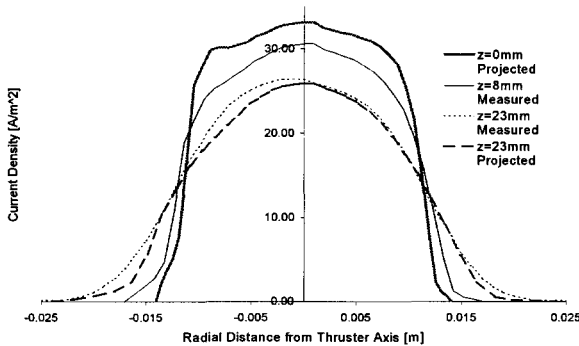


Figure 2. Projected Exit Plane Beam Profile

### Chamber Ion Density Profiles

Using the beam profile at the grid exit plane, the ion density profile just inside the chamber was approximated with the 2-D ion optics code, CEX2D. For each run the code gives beamlet currents for a range of chamber densities with a given grid geometry. Runs at multiple grid spacing values were performed to allow the effects of grid deflection to be considered. The relationship of between ion density and beam current generated by the code for a range of micro-ion grid spacing, and at the operating

conditions used to generate the data in Figure 1, is shown in Figure 3.

The results shown in Figure 3 were used to generate multiple linear relationships between ion density and beamlet current. The slopes of these

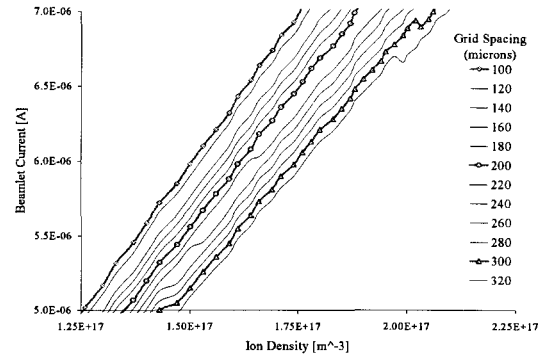


Figure 3. Chamber Ion Density vs. Beamlet Current for 100µm to 320µm Grid Spacing

relationships were then determined to be a function of grid spacing so that the ion density was expressed as a function of grid spacing and beamlet current. The resulting expression was used to generate ion density profiles from the exit plane beam profiles and the grid deflection data. The ion profile corresponding to the exit beam profile in Figure 2 is shown in Figure 4. Both profiles are normalized to show the degree of correlation. Since the data in Figure 3 was interpreted with a linear relationship, it is clear that the variation in the normalized profiles is due to the radial variation in grid spacing only. The approximation of grid deflection used for the data in Figure 4 approximated close to a 50% maximum decrease in grid spacing at the center of the grids.

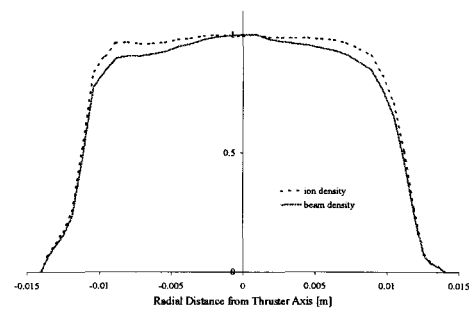


Figure 4. Normalized Ion Density Profile and Exit Plane Beam Density Profile

The code also calculates typical ion trajectories and the potential profile at the highest ion density for a given run. This information can be used to determine the ion optical properties of for a given grid geometry. For example, if large accelerator grid current is predicted by the code then the trajectories

and potential profiles will reveal whether this current is due to crossover or direct impingement current to the accelerator grid. Since low accelerator grid currents were experimentally measured, the beamlets for this investigation were considered to be sufficiently focused to avoid crossover or direct impingement currents. Figure 5 shows trajectory profiles for a micro-ion beamlet at grid spacing values of 300 $\mu\text{m}$  and 160 $\mu\text{m}$ . Figures 3 and 5 show that closer spacing typically results in greater beamlet current but can yield greater beamlet divergence.

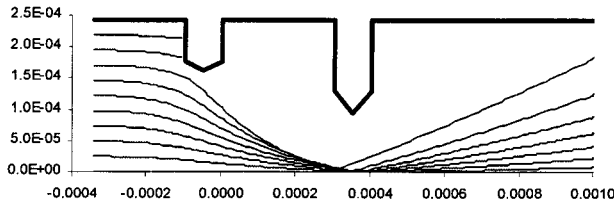


Figure 5a. Ion Trajectories for 300 $\mu\text{m}$  Grid Spacing

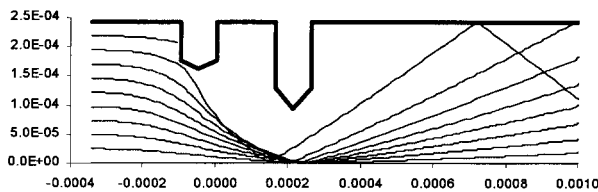


Figure 5b. Ion Trajectories for 160 $\mu\text{m}$  Grid Spacing

### Grid Utilization

The flatness parameters for the exit beam and ion profiles in Figure 4 are 0.597 and 0.632, respectively. Similar values were obtained for other operating conditions. These data show that the chamber design used for the micro-ion thruster produces desirable ion and beam profiles for the operation ranges investigated in this paper.

The projected ion densities were typically on the order of  $2.0 \times 10^{17} \text{ m}^{-3}$ , while the neutral densities were calculated using Equation (10) to be approximately  $2.0 \times 10^{20} \text{ m}^{-3}$ . The neutral loss rate, in equivalent amperes, was typically about half the beam current. The neutral densities and loss rates are greater than originally expected while the ion densities are lower than expected. These data show potential for improvement in thruster efficiency by methods such as: lowering accelerator grid open area fraction, lowering propellant flow rate, increasing the magnetic field strength, or any combination thereof. Preliminary runs of CEX2D show that a decrease in

accelerator hole size will likely yield favorable results.

### Conclusions

The micro-ion thruster design investigated herein yields favorable beam and ion profiles that show the magnetic field within the chamber efficiently uses the full radial extent of the exit grids. The high neutral density values in the chamber and preliminary calculations using small accelerator grid holes show that substantial increases in thruster efficiency are possible. The strong correlation of neutralizer emission current with the beam profile data helps to validate the data in Reference 2.

A quantitative correlation between ion and beam profiles is possible. Using the results of CEX2D the ion density may be expressed as a function of beam density and grid spacing. This result assumes adequate focusing of the beamlets. If crossover and direct impingement current to the accelerator grid is encountered, then the correlation is much less clear. The results show that closer grid spacing, with proper focusing, can result in greater beamlet current and divergence. A more accurate correlation of ion and beam density may be achieved if the angular deflection of the grids in the z-direction can be incorporated into CEX2D.

### Future Work

Modifications to the existing thruster design, such as smaller accelerator grid holes and stronger magnetic fields, will be considered. Due to the large grid deflection calculated herein, dished grids are being considered to stand off greater grid voltage differentials and to allow optimal spacing through the radial extent of the grids. Flight-worthy cathode design such as hollow and field emitter array (FEA) cathodes will be used in future test.

A computer model of the discharge chamber is being developed to help determine what modifications to the existing design will yield the best performance.

### Acknowledgements

The authors would like to acknowledge the indispensable help provided by Al Owens, John Brophy, Ira Katz, and John Ziemer.

### References

- [1] – Mueller, J., et al., “An Overview of MEMS- Based Micropropulsion Developments at JPL,” IAA Paper B3-1004, 3<sup>rd</sup>

International Symposium on Small Satellites for Earth Observation, International Academy of Astronautics (IAA), Berlin, Germany, April 2001

[2] – Wirz R., Polk J., Marrese C., Mueller J., Escobedo J., Sheehan P., “Development and Testing of a 3cm Electron Bombardment Micro-Ion Thruster,” IEPC Paper 01-343, 27<sup>th</sup> IEPC, Pasadena, CA, Oct 2001

[3] – Wilbur P. J., “Correlation of Ion and Beam Current Densities in Kaufman Thrusters,” Journal of Spacecraft and Rockets, Vol. 10, No. 9, Sept. 1973, pp 623-624

[4] – Knauer W., Poeschel R. L., Ward J. W., “Radial Field Kaufman Thruster,” Journal of Spacecraft and Rockets, Vol. 7, No. 3, March 1970, pp. 248-251

[5] – Parks D. E., Katz I., “Preliminary Model of Ion Beam Neutralization,” Electric Propulsion and Its Applications to Space Missions, Finke R. C. editor, Progress in Astronautics and Aeronautics Vol. 79, AIAA 1981

[6] – Shunk D. D., “Finite Element Analysis of Ion Thruster Grids,” Thesis, Colorado State University, Fort Collins, CO, Spring 2002

[7] – Lih M. S., “Parametric Study of the Structural Response of Carbon/Carbon Ion Grids,” JPL Internal Document, May 2, 2001

[8] – Beattie, J. R., “Cusped Magnetic Field Mercury Ion Thruster,” NASA-CR – 135047, July 1976

[9] – Brophy, J. R., “Ion Thruster Performance Model,” NASA-CR-174810, December, 1984

[10] – Schott, L., “Electric Probes,” Plasma Diagnostics, Lochte-Holtgreven W. editor, North-Holland, 1968, APS 1995